Molecular Dynamics Study on Microheterogeneity and Preferential Solvation in Methanol/Chloroform Mixtures

R. Gratias and H. Kessler*

Institute of Organic Chemistry and Biochemistry, Technical University Munich, Lichtenbergstr. 4, D-85747 Garching, Germany

Received: July 15, 1997; In Final Form: October 29, 1997

Molecular dynamics simulations have been used to study the structure and properties of methanol/chloroform mixtures with varying molecular fractions. The results of the simulations of the neat liquids have been validated by comparing the calculated radial distribution functions with those previously published. Experimental and calculated densities of the mixture at various molar ratios were in very good agreement. The analysis of radial distribution functions of the mixtures at different concentrations revealed clustering effects in the solvent mixture. To provide a more detailed insight into this phenomenon, local molecular fractions at varying distances are presented that clearly show these clustering effects. It was also demonstrated, that in such a mixture hydrophilic and hydrophobic parts of amphiphilic solutes are preferentially solvated by methanol or chloroform, respectively.

Introduction

Lipophilic and amphiphilic molecules exhibit remarkable solubility in mixtures of methanol and chloroform. This solvent system is often used in synthesis, chromatography, and spectroscopy of such molecules because of their remarkable solubility. In high-resolution NMR spectroscopy of membrane-bound compounds, mixtures of methanol and chloroform function as isotropic membrane mimics.[1−4] For example, it has been shown that transmembrane α-helical peptides derived from bacteriorhodopsin exhibit similar structures in anisotropic SDS micelles and in isotropic methanol/chloroform mixtures.[1] Because the transmembrane protein EmrE[5] maintains its activity after dissolving in a mixture of methanol and chloroform,[6] the solution structure of EmrE in this solvent system is currently being investigated in our group by NMR techniques. In studies where an anisotropic environment is mimicked by an isotropic one, it is of special interest to gain detailed insight about the solvate structure around the solute.

However, this solvent system is not only interesting from the practical point of view, but some theoretical aspects of this problem are also remarkable. Methanol and chloroform are completely miscible in all ratios. This miscibility is in strong contrast to the apparently very similar solvent pair of water and chloroform, which are essentially immiscible. There are some interesting thermodynamic features associated with methanol and chloroform[7] which have a major influence on understanding structural aspects in these systems. It is well-known that mixtures of simple alcohols with nonpolar solvents show large positive deviations from Raoult's law.[8] These deviations are usually interpreted in terms of heterogeneity at a microscopic level[9,10] and self-association of the alcohol molecules.[8] It is also well-known that mixtures of chloroform with the lower aliphatic alcohols are far from regular.[11] The large negative excess entropy of methanol/chloroform mixtures has been attributed to homomolecular or perhaps even heteromolecular clustering.[12,13] In similar mixtures, such associations have been detected with other techniques, too; for example, in methanol/carbon tetrachloride systems, self-association has been observed by diffusion measurements[8] and nuclear magnetic relaxation techniques.[14,15]

To gain a better understanding of the structure and the properties of neat liquids, empirical forcefield methods such as molecular dynamics (MD) or Monte Carlo (MC) have proven to be useful.[16−23] Although aqueous mixtures also have attracted considerable attention,[24−28] systems containing simple organic solvents have only rarely been studied.[29,30] Therefore, it is of interest to determine whether MD calculations of methanol/chloroform mixtures also exhibit this clustering and whether these simulations are in agreement with experimental data. If self-association or clustering can be observed, it also raises further questions whether preferential solvation of solute molecules occurs in these solutions.[31,32] Considering the fact that methanol/chloroform mixtures are often used as membrane mimics, the use of amphiphilic molecules as probes is of special interest. These studies on small molecules would then allow further calculations of transmembrane peptides and proteins with an explicit solvation.

Computational Methods

All MD calculations were performed with the MSI program suite Discover and the CVFF forcefield[33] (without cross terms or Morse potentials) on SGI Indy workstations or an IBM SP2. For the subsequent analysis of the trajectories, the MSI programs InsightII and Decipher were used.

For MD calculations, a leapfrog Verlet integrator algorithm[34] with 1 fs time steps was used. During temperature scaling processes, the temperature was adjusted by the fast and efficient direct velocity scaling algorithm,[35] whereas a more gentle Berendsen temperature bath coupling[36] (temperature relaxation time $\tau_T = 0.1$ ps) was used during equilibration and production phases. The pressure adjustment to 1 bar in NPT (constant

* Author to whom correspondence should be sent. Tel: ++49+89/289-13300, Fax: ++49+89/289-13210. E-mail: kessler@artus.org.chemie.tu-muenchen.de.

S1089-5647(97)02295-5 CCC: $15.00
Published on Web 02/25/1998

TABLE 1: Forcefield Parameters for Methanol and Chloroform

methanol			
bond	K_b [kcal/mol Å^2]		b_0 [Å]
C−O	384.0		1.430
O−H	540.6		0.945
angle	K_Θ [kcal/mol rad^2]		Θ_0 [deg]
C−O−H	58.5		108.5
Lennard-Jones parameter	σ [Å]	ϵ [kcal/mol]	charge
C	3.775	0.207	0.265
O	3.070	0.170	−0.700
H	0.0	0.0	0.435
chloroform			
bond	K_b [kcal/mol Å^2]		b_0 [Å]
C−Cl	314.0		1.758
angle	K_Θ [kcal/mol rad^2]		Θ_0 [deg]
Cl−C−Cl	85.0		111.3
pseudo dieder	K_ϕ [kcal/mol]	ϕ_0 [deg]	n
Cl−*C*−Cl−Cl	10.0	−55.22	1
Lennard-Jones parameter	σ [Å]	ϵ [kcal/mol]	charge
C	3.800	0.080	0.420
Cl	3.470	0.300	−0.140

number of particles, pressure, temperature) ensembles was achieved with an analogous pressure bath coupling (pressure relaxation time $\tau_P = 0.1$ ps, isothermal compressibility $\beta = 5.0 \times 10^{-5}$ bar^{-1}).[36]

Minimum image convention[18] was used for the cubic periodic boundary systems, with an initial simulation box length of 36 Å. Long-range, nonbonded energy contributions were calculated according to a charge group concept (each solvent molecule as a charge group) up to a distance of $r = 16.5$ Å. To smoothly turn off these interactions, a switching function to zero (fifth order polynomial) was applied in the interval 15.5 Å $< r \leq$ 16.5 Å.

For nonbonded energies, a normal 12−6−1 Lennard-Jones type pair potential

$$V = \sum_{i<j} \frac{A_{ij}}{r_{ij}^{12}} - \frac{B_{ij}}{r_{ij}^{6}} + \frac{q_i q_j}{4\pi\epsilon_0 r_{ij}}; A = 4\epsilon\sigma^{12}; B = 4\epsilon\sigma^{6}$$

with geometric combining rules ($A_{ij} = (A_i A_j)^{1/2}$, $B_{ij} = (B_i B_j)^{1/2}$) for the parameters of nondiagonal interactions was used. The difference in the results obtained using these combining rules and the well-known Lorentz−Berthelot rules[18]

$$\sigma_{ij} = {}^1/_2(\sigma_i + \sigma_j),\ \epsilon_{ij} = (\epsilon_i\,\epsilon_j)^{1/2}$$

is negligible.[30]

The three-site potential model for methanol, treating the methyl group as an united atom, has been derived from Jorgensen's OPLS forcefield,[19,21] and each molecule was treated as flexible. Parameters for the internal degrees of freedom have been deduced from similar structural elements in the CVFF forcefield. An analogous procedure yielded the four-site model for chloroform.[37−39] (see Table 1).

The simulation systems of the mixtures have been generated by soaking a cubic box (36 Å)^3 with layers of the corresponding volumetric parts of preequilibrated neat solvents (*V*(MeOH)/*V*(CHCl$_3$): 0/1, 1/2, 1/1, 2/1, 1/0). To ensure a proper mixing process, a special equilibration protocol has been developed in which the coordinates of all atoms in the initial solvent box are first randomized. Correct molecule geometries were then obtained by minimizing the potential energy within 10 cycles of steepest descent optimization (2000 iterations each), scaling the van der Waals (vdW) radius with an increasing factor of 0.0 to 1.0. During the first six cycles, a quartic potential for nonbonded vdW interactions was chosen. Subsequently, temperature was increased to 300 K in 1 ps steps of 50 K. Equilibration in an NPT ensemble at 300 K was completed within 300 ps at the latest. Because it was one of our goals to obtain preequilibrated solvent systems that include solute interactions, these solvent systems were not analyzed further. Instead, new simulation boxes ((36 Å)^3) were soaked with the compounds of these equilibrated mixtures (see Table 2). Subsequently, an analogous minimizing, heating, and equilibration protocol without randomization and vdW radius scaling was used. As an example for the equilibration process, time histories of the total energy and the density of the mixture 2/1 (see Table 2) are shown in Figure 1. For analysis, 100 ps, with snapshots every 0.1 ps, were collected.

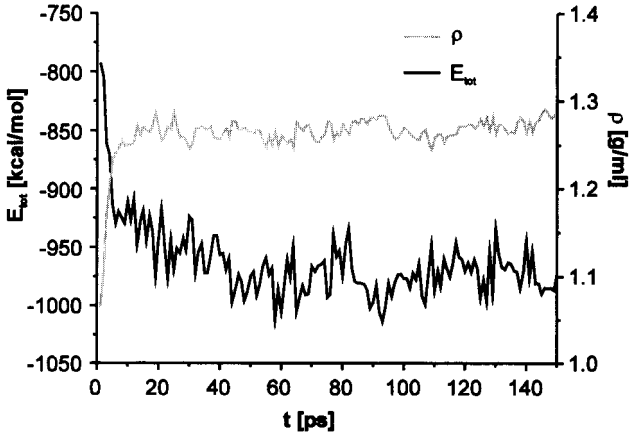

Figure 1. Time history of the total energy and the density during the equilibration of the mixture with the volumetric fraction 2/1.

TABLE 2: Analyzed Solvent Systems: Volumetric Parts, Molar Fractions, and Number of Simulated Molecules

V(CHCl$_3$)/*V*(MeOH)	1/0	2/1	1/1	1/2	0/1
X (CHCl$_3$)	1.00	0.60	0.33	0.21	0.00
N (CHCl$_3$)	288	209	144	97	0
N (MeOH)	0	140	295	360	668

To study preferential solvation processes, the same procedure was applied. Because it was the intention to investigate the behavior of the solvent, the test solute molecules were kept rigid at a potential energy minimum. The only exception was sodium palmitate, for which the coordinates of the Na^+ ion were not fixed.

Results and Discussion

In an initial step it was necessary to determine whether the implementation of the potentials for flexible particles induces artifacts, because the solvent molecules were originally constructed as rigid. Therefore, various radial distribution functions (rdf's) of pure methanol[21] and chloroform[29] were compared with those found in the literature. In methanol, perhaps most interesting is the rdf g_{OH}, which describes the hydrogen bonding. The rdf has a maximum at 1.77 Å, with a coordination number to the first minimum at 2.53 Å of 0.98, compared with a maximum at 1.77 Å with 1.01 neighbors up to 2.48 Å. The

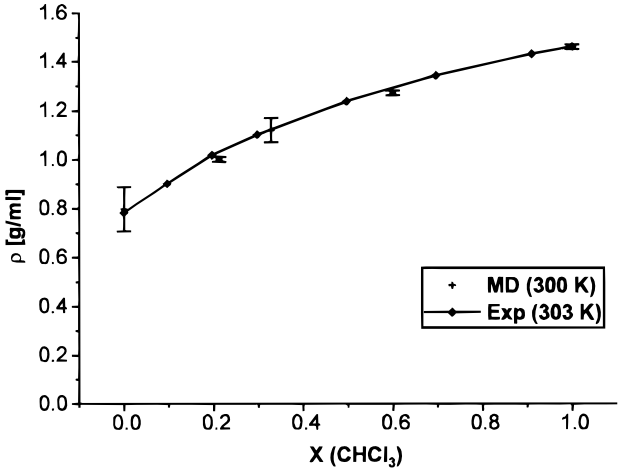

Figure 2. Comparison of experimental (see text) and calculated densities. The experimental values (Exp 303K) are represented by the diamonds and the continuous curve. The calculated densities (MD 300K) are shown as crosses containing error bars.

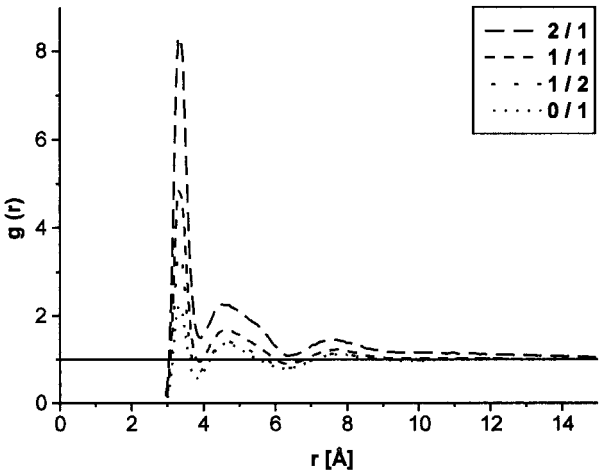

Figure 3. Comparison of the rdf's of methanol at different molar fractions. The volumetric fractions (2/1, 1/1, 1/2, 0/1) are listed in Table 2.

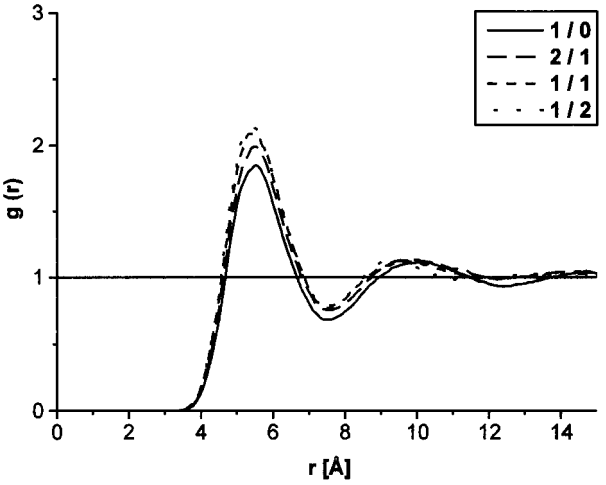

Figure 4. Comparison of the rdf's of chloroform at different molar fractions. The volumetric fractions (1/0, 2/1, 1/1, 1/2) are listed in Table 2.

g_{OO} exhibits a peak at 2.70 Å in our calculations and 2.70 Å in Jorgensen's calculation. For chloroform, a comparison of the broad maximum of g_{CC} yields 5.4 Å for our simulations versus 5.3 Å in the literature, with a coordination number to the top of the maximum of 3.6 and 3.0, respectively. Although only some representative examples are shown here, in general the rdf's are in good agreement (further data not shown).

The solvent mixture models have been validated by comparing the densities produced in the NPT ensemble at various molecular fractions with experimental ones.[40] As illustrated in Figure 2 the results from the calculations are in excellent agreement with the experimental results. We would also like to point out that the excess volume of mixing of methanol and chloroform was also nicely reproduced by our simulations. Because the mixing protocol starts from equilibrated, neat solvent models that exhibit the correct density, the decrease of the volume during the simulation to the correct density is in accordance with the volume reduction during a real mixing process.

Structural changes within mixtures of different molar fractions should result in significant alterations in the rdf's. Therefore, a variety of rdf's at different mixing ratios were calculated. The rdf's that correspond to the distribution of the whole molecule are depicted in Figures 3 and 4. From these it is quite obvious that, compared with the neat solvents, the position of maxima and minima on the r-axis for methanol and chloroform remained constant. The variation of the coordination number up to the first minimum is also negligible for methanol ($\pm$ 0.15). As indicated by the distribution function g_{OH} (data not shown), this results from hydrogen bonding between a hydrogen atom and an oxygen atom at a distance of 1.8 Å. For longer distances, the coordination number rises with higher concentrations. Similarly, the number of neighbors in g_{CHCl_3} grows almost linear with the molecular fraction. Nevertheless, the peak intensities of the rdf's of chloroform rise slightly with lower chloroform concentrations, but the intensities of g_{MeOH} increase dramatically if the methanol concentration is lowered. For example, g_{MeOH} of the first maximum rises from 2.2 in pure methanol to 8.3 in the solution with the lowest methanol content (X(MeOH) = 0.40). That increase holds not only true for the first maximum, but for the whole distance range out to 10 Å. As the rdf's are normalized to the global molecular fraction within the mixture, this observation corresponds on a microscopic level to a higher concentration of methanol molecules around another methanol molecule than the global molecular fraction might suggest.

To characterize this phenomenon in more detail, the local molecular fraction X_{loc}[29] was calculated as a function of the distance to the corresponding test molecule. The local molecular fraction $X_{loc,A}$ of compound A in a binary mixture A/B is defined as $X_{loc,A}(r) = N_{AA}(r)/(N_{AA}(r) + N_{AB}(r))$, where $N_{AX}(r)$ is the number of molecules X at a distance r from molecule A. The results are shown in Figures 5 and 6. Due to the large molecular diameter of chloroform, all values with a distance lower than 4−5 Å contain artificial distortions.

In a homogeneous mixture, no significant deviations of X_{loc} from the global molecular fraction is expected. However, compared with the global molecular fraction, the local molecular fraction of methanol is strongly increased up to a distance of ~10 Å. In addition, with lower content of methanol in the solution, this difference is higher. It is interesting to note that not only for methanol, but also for chloroform, a higher X_{loc} has been observed for distances <10 Å. These increased local molecular fractions of both compounds must be the result of clustering effects in the liquid. Although the changes of the chloroform rdf's are only minor, the local molecular fractions clearly reveal the clustering of methanol and chloroform. Based

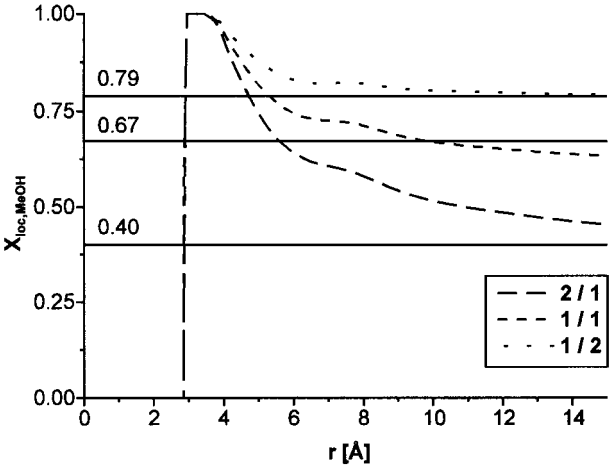

Figure 5. Local molecular fraction $X_{loc,MeOH}$ of methanol as a function of the distance. Horizontal lines indicate the global molecular fraction. The volumetric fractions (2/1, 1/1, 1/2) are listed in Table 2.

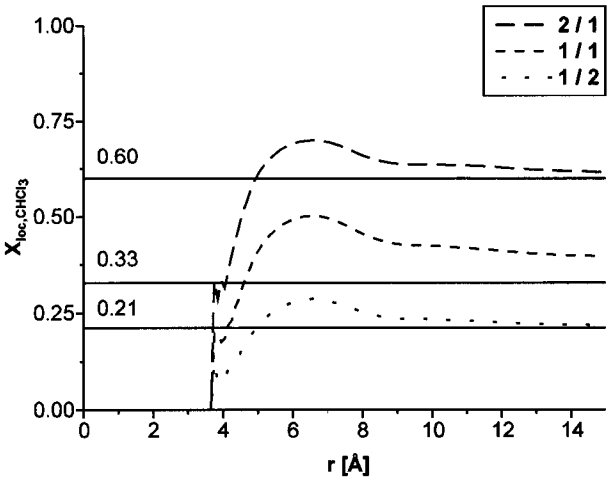

Figure 6. Local molecular fraction $X_{loc,CHCl_3}$ of chloroform as a function of the distance. Horizontal lines indicated the global molecular fraction. The volumetric fractions (2/1, 1/1, 1/2) are detailed in Table 2.

on our results, the size of these clusters is in the range of 10 Å. These clusters within the simulation box can easily be recognized in the snapshots of the MD trajectory shown in Figure 7.

To investigate the influence of a solute on the structure of the solvent mixture, especially preferential solvation processes, the three amphiphilic molecules dimyristoylphosphatidylcholine (DMPC), sodium palmitate, and palmitoyl amide have been used as test molecules. In Figure 8 a graphical representation of the number of methanol molecules within a 7 Å sphere around each heavy atom of the test molecule is shown. For chloroform (not depicted here), the distribution is reversed. As can be seen clearly, the highly charged atoms (whether positive or negative) in the phosphatidylcholine group of DMPC and the sodium carboxylate moiety of sodium palmitate are mainly surrounded by methanol. The carboxamide in palmitoyl amide only shows a slight preference for methanol. In contrast, the alkyl groups of all investigated molecules favor a chloroform-rich environment. Obviously, an alignment of either methanol or chloroform clusters at the scaffold of the solute according to the hydrophilicity is induced.

Conclusion

Empirical forcefield calculations have been used to obtain a better understanding of the properties of liquids at the molecular level. Here, the calculations of methanol/chloroform mixtures

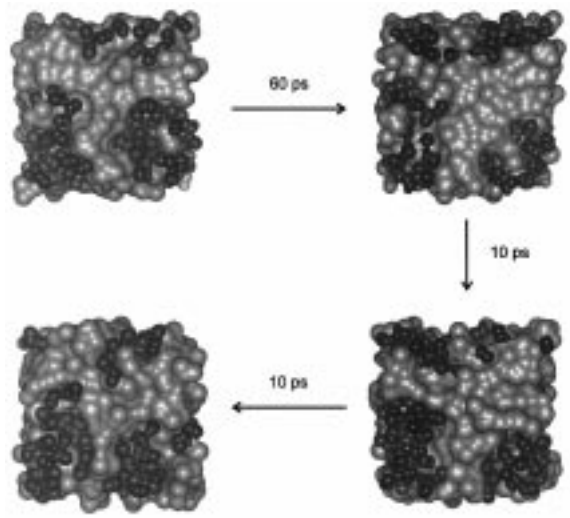

Figure 7. Snapshots of the MD trajectory for the 1/1 mixture showing the variation of the clusters in the mixture. For chloroform a Connolly surface (probe radius: 2 Å) is used; for methanol a CPK representation.

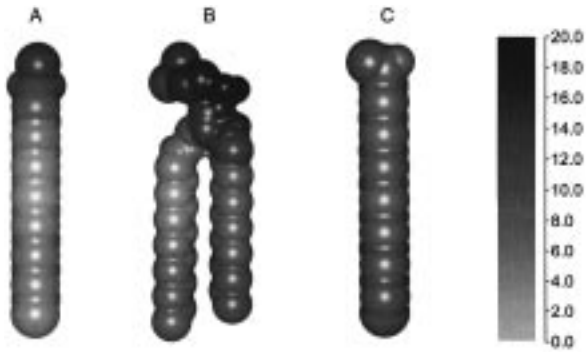

Figure 8. Methanol distribution around sodium palmitate (A), DMPC (B), and palmitoyl amide (C). The functional groups with the highest partial charges are positioned at the top of the figure. The spectrum represents the number of methanol molecules within a sphere of 7 Å around the selected heavy atom.

in NPT ensembles yielded a very good agreement between experimental and theoretical densities.

The simulations showed self-association and clustering within these liquids. The increase of the local molecular fractions up to a distance of 10 Å are a result of association processes, which have already been suggested based on results from thermodynamic experiments.[11−13] It is interesting to note that not only for methanol, but also for chloroform, self-association has been found.

The clustering might be the basis for the observed preferential solvation and therefore the reason for the interesting solvent properties of these systems. Regardless of what kind of solute (hydrophobic or hydrophilic) is dissolved in this mixture, it is always solvated by corresponding solvent molecules. For example, the lipophilic parts of membrane proteins can be solvated by chloroform and the hydrophilic parts by methanol. In addition, the results obtained with the amphiphilic test molecules encourage us to use the solvent model presented here for further MD simulations of transmembrane peptides and proteins, which are currently under investigation by high-resolution NMR.

Acknowledgment. The financial support of this research by the DFG is gratefully acknowledged. We would also like to thank the LRZ Munich for providing computer time on the IBM SP2.

References and Notes

(1) Pervushin, K. V.; Arseniev, A. S. *FEBS* **1992**, *308*, 190−196.
(2) Barsukov, I. L.; Nolde, D. E.; Lomize, A. L.; Arseniev, A. S. *Eur. J. Biochem.* **1992**, *206*, 665−672.
(3) Orekhov, V. Yu.; Abdulaeva, G. V.; Musina, L. Yu.; Arseniev, A. S. *Eur. J. Biochem.* **1992**, *210*, 223−229.
(4) Pervushin, K. V.; Orekhov, V. Yu.; Popov, A. I.; Musina, L. Yu.; Arseniev, A. S. *Eur. J. Biochem.* **1994**, *219*, 571−583.
(5) Yerushalmi, H.; Lebendiker, M.; Schuldiener, S. *J. Biol. Chem.* **1995**, *270*, 6856−6863.
(6) Schuldiner, S.; Lebendiker, M.; Yerushalmi, H. *J. Exp. Biol.* **1997**, *200*, 335−341.
(7) Naberukhin, Yu. I.; Rogov, V. A. *Russ. Chem. Rev.* **1971**, *40*, 207−215.
(8) Prabhakar, S.; Weingärtner, H. *Z. Phys. Chem. Neue Folge* **1983**, *137*, 1−12.
(9) Mills, R.; Hertz, H. G. *J. Phys. Chem.* **1980**, *84*, 220−224.
(10) Patterson, D. *J. Solution Chem.* **1994**, *23*, 105−120.
(11) A regular solution is defined as one in which the excess entropy is zero. Scatchard, G.; Raymond, C. L. *J. Am. Chem. Soc.* **1938**, *60*, 1278−1287.
(12) Moelwyn-Hughes, E. A.; Missen, R. W. *J. Phys. Chem.* **1957**, *61*, 518−521.
(13) Singh, P. P.; Sharma, B. R.; Sidhu, K. S. *Can. J. Chem.* **1979**, *57*, 387−393.
(14) Koch, W.; Leiter, H.; Mal, S. *Z. Phys. Chem. Neue Folge* **1983**, *136*, 89−99.
(15) Wandler, U.; Hertz, H. G. *Z. Phys. Chem. Neue Folge* **1992**, *178*, 217−228.
(16) Rossky, P. J. *Annu. Rev. Phys. Chem.* **1985**, *36*, 321−346.
(17) Ladanyi, B. M.; Skaf, M. S. *Annu. Rev. Phys. Chem.* **1993**, *44*, 335−368.
(18) Allen, M. P.; Tildesley, D. J. *Computer Simulation of Liquids*; Clarendon Press: Oxford, 1987.
(19) Jorgensen, W. L.; Maxwell, D. S.; Tirado-Rives, J. *J. Am. Chem. Soc.* **1996**, *118*, 11225−11236.
(20) Jorgensen, W. L. *J. Phys. Chem.* **1986**, *90*, 1276−1284.
(21) Jorgensen, W. L. *J. Am. Chem. Soc.* **1980**, *102*, 543−549.
(22) Liu, H.; Müller-Plathe, F.; van Gunsteren, W. F. *J. Am. Chem. Soc.* **1995**, *117*, 4363−4366.
(23) Rahman, A.; Stillinger, F. H. *J. Chem. Phys.* **1971**, *55*, 3336−3359.
(24) Skaf, M. S.; Ladanyi, B. M. *J. Phys. Chem.* **1996**, *100*, 18258−18268.
(25) Kovacs, H.; Laaksonen, A. *J. Am. Chem. Soc.* **1991**, *113*, 5596−5605.
(26) Suwannachot, Y.; Hannongbua, S.; Rode, B. M. *J. Chem. Phys.* **1995**, *102*, 7602−7609.
(27) Freitas, L. C. G.; Cordeiro, J. M. M. *J. Mol. Struct. (THEOCHEM)* **1995**, *335*, 189−195.
(28) Hawlicka, E. *Pol. J. Chem.* **1996**, *70*, 821−837.
(29) Kovacs, H.; Kowalewski, J.; Laaksonen, A. *J. Phys. Chem.* **1990**, *94*, 7378−7385.
(30) Sinoti, A. L. L.; dos Santos Politi, J. R.; Freitas, L. C. G. *J. Mol. Struct. (THEOCHEM)* **1996**, *366*, 249−258.
(31) Marcus, Y. *J. Chem. Soc., Faraday Trans.* **1989**, *85*, 381−388.
(32) Bagno, A.; Scorrano, G.; Stiz, S. *J. Am. Chem. Soc.* **1997**, *119*, 2299−2300.
(33) Dauber-Osguthorpe, P.; Roberts, V. A.; Osguthorpe, D. J.; Wolff, J.; Genest, M.; Hagler, A. T. *Proteins: Struct., Funct., Genet.* **1988**, *4*, 31−47.
(34) Verlet, L. *Phys. Rev.* **1967**, *159*, 98−103.
(35) *Discover User Guide*; Biosym/MSI: San Diego, 1995.
(36) Berendsen, H. J. C.; Postma, J. P. M. van Gunsteren, W. F.; DiNola, A.; Haak, J. R. *J. Chem. Phys.* **1984**, *81*, 3684−3690.
(37) Jorgensen, W. L.; Boudon, S.; Nguyen, T. B. *J. Am. Chem. Soc.* **1989**, *111*, 755−757.
(38) Jorgensen, W. L.; Briggs, J. M.; Contreras, M. L. *J. Phys. Chem.* **1990**, *94*, 1683−1686.
(39) Jen, M.; Lide, J. R. *J. Chem. Phys.* **1962**, *36*, 2525−2526.
(40) Crabtree, A. M.; O'Brien, J. F. *J. Chem. Eng. Data* **1991**, *36*, 140−142.